MODELLING OF MECHANICAL PROPERTIES OF RANDOMLY ORIENTED STRANDS THERMOPLASTIC COMPOSITES

M. Selezneva[a], S. Meldrum[a], S. Roy[b], L. Lessard[a*], A. Yousefpour[b]

[a]*Department of Mechanical Engineering, McGill University, 817 Sherbrooke st. West, Montreal, QC, Canada, H3A 0C3*
[b]*National Research Council Canada, 5145 Decelles ave., Montreal, QC, Canada H3T 2B2*
**Larry.Lessard@mcgill.ca*

Keywords: randomly oriented strands, thermoplastics, mechanical properties

Abstract

Randomly oriented strands (ROS) thermoplastic composites have attractive properties, such as great formability and high modulus, but their properties are highly variable due to heterogeneous macrostructure. This paper proposes a stochastic finite element technique that predicts strength and modulus of ROS composites. It is based on the concept of random strands generation to model variability, and it utilizes Hashin's failure criteria and fracture energies to estimate strength. Overall, the model matches experimental results and shows that failure of ROS composites is matrix-dominated and follows the "weakest-link" principle.

1. Introduction

There is an emerging interest in the aerospace industry in manufacturing components with intricate features, such as complex parts with ribs and thickness variations, using discontinuous-fibre composite materials. The conventionally used continuous fibre (CF) composites are difficult to form, while the short fibre preforms used by the automotive industry lack the required mechanical properties. Material systems with long discontinuous fibres and high fibre volume fraction have the potential of filling the niche between the formability of short fibre preforms and the performance of CF composites. A candidate material system is composed of randomly-oriented-strands (ROS) that can be used in compression moulding, as shown in Figure 1. ROS composites were found to be an attractive alternative to metals since they do not corrode, are lighter and cheaper to manufacture [1]. However, only a limited number of studies found in the open literature discuss processability and mechanical properties of these materials. A new multi-disciplinary study [2-6] is being conducted to systematically characterize and model the moulding process and mechanical properties of composites manufactured from carbon/Polyether ether ketone (PEEK) ROS.

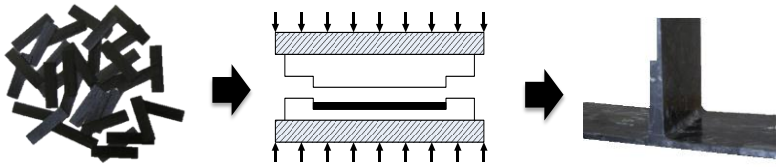

Figure 1. Manufacturing process of ROS parts

2. Literature review

Recent studies investigated mechanical properties [7-10], demonstrated design potential [1, 7, 11] and proposed modelling techniques [7, 12, 13] for ROS composites. One of the issues associated with this material system is its heterogeneity, which gives rise to large variability. To capture the variability of modulus, Sato *et al.* [12] and Feraboli *et al.* [13] proposed modelling schemes, in which a specimen was discretized into regions (or elements) with different ply layups, and hence different properties. Localized modulus was calculated by applying the classical laminate theory to each element. Global modulus of the entire specimen was calculated by either analytically superimposing the effect of local moduli in the widthwise and lengthwise directions [12] or by modelling the specimen in a finite element (FE) software [13]. The latter method is shown in Figure 2. These approaches were able to capture the average modulus and its variability. However, since there are no actual repeating units, it is difficult to choose an appropriate size for a representative element. The use of large elements, whose layups are completely random and not dependent on the neighbouring elements, leads to large variation of properties across the element boundaries and large strain discontinues, as shown in Figure 2b.

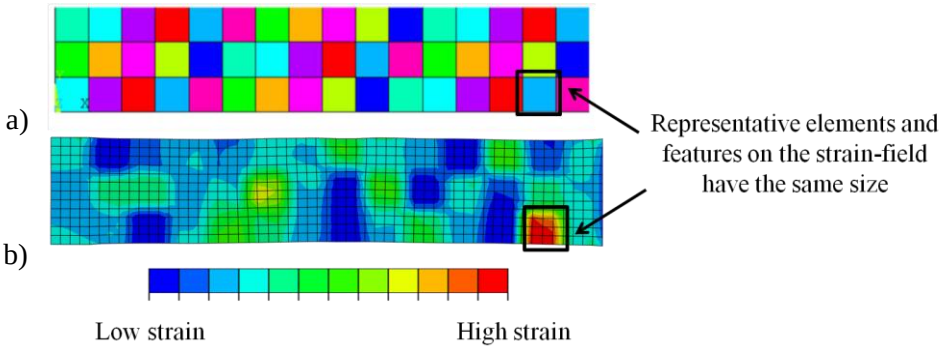

Figure 2. a) Model of an ROS composites proposed by [13] in which a specimen is subdivided into regions with different properties (shown with different colours) and b) the resultant strain-field under loading (colour map corresponds to strain variability)

3. Modelling

3.1. Scope and assumptions

The main goal of this paper is to propose a modelling technique that captures the variability of strength and modulus of ROS composites. Results were compared against experimental work, which encompasses testing of CF laminates and ROS composites with different strand sizes (12 – 50 mm long and 6 mm wide). The modelling technique has three modules: 1) generating random strand layup for a specimen, 2) building a finite element model and 3) analyzing its stress-strain response. In contrast to the previous models, small partitions were used for discretization, hence improving continuity of properties among the neighbouring regions. At this stage, a simple 2D model was used, which ignores the following:

- strand out-of-plane orientation and waviness,
- interlaminar shear between strands,
- stress concentrations at strand ends,
- residual thermal stresses.

These factors are not negligible and will need to be accounted for in the future versions of the model.

3.2. Randomization algorithm and laminate analogy

An algorithm was written in MATLAB to create a "specimen" with variable properties by generating strands with random orientations and placing them at random locations within that "specimen". This randomly generated specimen is unique and will be referred to as an FE specimen. This process is illustrated in Figure 3. Each FE specimen is discretized into an array, termed as specimen-array in this paper, which stores the number of plies and their orientation. Each element in this array is referred to as a partition, in order to avoid confusion with mesh elements in the FE model. Each partition represents a region of a specimen with distinct properties. For each strand randomly created, it is assigned a position within the FE specimen and an orientation. If a portion of the strand protrudes outside of the FE specimen, it is cut off and is not reinserted from the other side (i.e. "torus conversion" is not used). In the end, each partition in the specimen-array contains the layup information. Symmetry and balance of the layup are not enforced during strand generation. Since flow of the material is not considered and no restriction is applied on strand location, the number of strands varies from one partition to another. In order to achieve uniform thickness everywhere, the thickness of each "ply" in the partition is scaled such that total thickness is constant (in this case 2.5 mm).

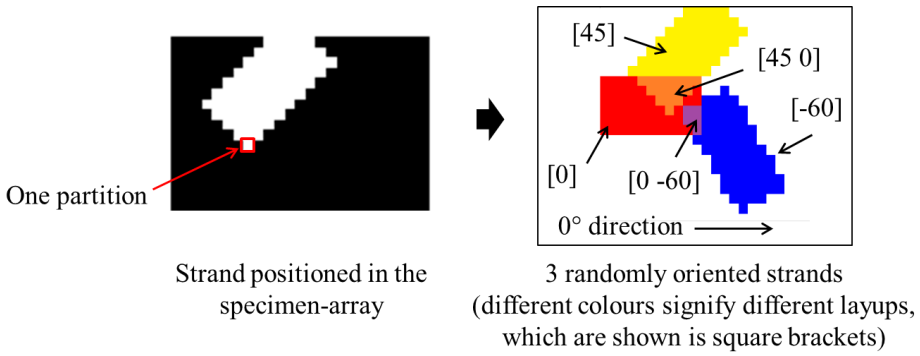

Figure 3. Strand generation algorithm

3.3. Finite element model

Finite element model was created in ABAQUS to evaluate the stress-strain response of the material. A Python script was used to generate the model (geometry, boundary conditions, *etc*.) and to assign layups from the specimen-array to each partition in the FE specimen. The mesh size has to be the same as the partition size or finer, and each mesh element has to be fully within a partition (i.e. it cannot be split between two partitions with different properties). The modelled geometry corresponds to the gauge section of an actual tensile specimen, which is 25 x 150 mm^2. For simplicity, the same mesh and partition size were used, such that each element was 1 x 1 mm^2 and had its own layup. The effect of mesh and partition size will be discussed in the results section. The FE specimen was modelled using 4-node quad shell elements (S4). The stress-strain curve was captured by incrementally applying a displacement and measuring the force resultants. The complete set of boundary conditions is shown in Figure 4.

Damage initiation was determined by the Hashin's failure criteria [14], which were chosen due to their ease of implementation since they are directly available in ABAQUS. Damage propagation was modelled by linearly softening the material (i.e. reducing the modulus) based on the concept of fracture energy dissipation [15]. This concept is depicted in Figure 5.

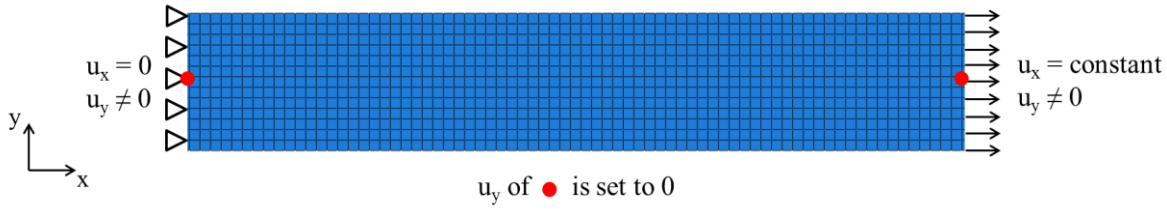

Figure 4. Boundary conditions imposed on the FE specimen. *X* and *Y* refer to longitudinal and transverse directions, and *u* represents displacement

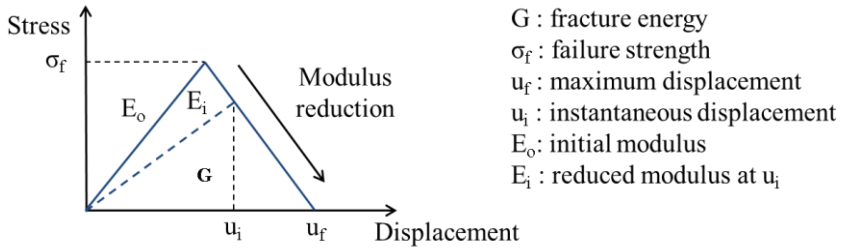

Figure 5. Modulus reduction as a function of fracture energy

Mechanical properties of carbon/PEEK are readily available from the manufacturer and are summarized in Table 1. No experimentally measured values for fracture energies of carbon/PEEK were found in the open literature. Benchmark values were taken from the paper by Naderi [16] and were then adjusted (Table 1) so that stress-strain curves of $[0/\pm60]_{3S}$ and $[90/\pm30]_{3S}$ CF laminates generated with FE models would match the experimental results.

In the case of ROS composites, ten simulations with different layups were run for each strand size, and failure was assumed to occur when the model failed to converge. Loading was applied incrementally with a constant step size, but as the element properties began to degrade and ABAQUS experienced difficulties with convergence, the step size was automatically reduced.

Material properties of AS4/PEEK		
Modulus [GPa]	Longitudinal	130
	Transverse	10
	In-plane shear	5.2
	Out-of-plane shear	3.759*
	Poisson's ratio	0.33
Strength [MPa]	Longitudinal tension	2280
	Longitudinal compression	1300
	Transverse tension and compression	86**
	In-plane shear	152
	Out-of-plane shear	94
Fracture energy [N/mm]	Longitudinal tension	1
	Longitudinal compression	1
	Transverse tension	10
	Transverse compression	10

Table 1. Mechanical properties of carbon/PEEK plies, as provided by the manufacturer; *Out-of-plane shear modulus was calculated based on the transverse isotropic assumption; and ** Transverse tension and compression strengths were assumed to be the same.

4. Experimental procedure

The material used was carbon/PEEK unidirectional tape. CF quasi-isotropic panels with $[0/\pm60]_{3S}$ layup and ROS panels with 12, 25 or 50 mm long strands were manufactured using compression moulding. Processing pressure and temperature were 35 bars and 380°C. More details are available in [2, 3]. CF panels were cut such that specimens had $[0/\pm60]_{3S}$ and $[90/\pm30]_{3S}$ fibre orientations. For each strand size, eight specimens were cut. Specimens were 250 mm long and 25 mm wide, and had a gauge section of 150 x 25 mm^2. During testing, strain was measured with the Digital Image Correlation (DIC) technique using a single 5 megapixel camera. Specimens were loaded in tension at 2 mm/min, and LVDT data and DIC images were captured at 5 Hz. Image analysis was performed using VIC-2D software (Correlated Solutions). Modulus was calculated by using average strain from each DIC image.

5. Results and discussion

A one-to-one comparison between the model and the experiments cannot be obtained since the exact strand orientation and placement in an ROS specimen are unknown and hence cannot be simulated. However, general trends can still be compared. Figure 6 shows evolution of the strain-field during loading of a) an actual and b) a randomly simulated ROS specimens. Both show that there are regions of high strain, which are noticeable even at low loads, while the rest of the specimen experiences significantly lower strains. The earlier model developed by Feraboli *et al*. [13] was also able to capture regions of high and low strain, but their size and shape depended on the partition size, which is shown in Figure 2. The current model captures the shape and size of these regions independently of the partition size, since each partition is a lot smaller than a single strand and the difference in modulus from one partition to another is not as drastic.

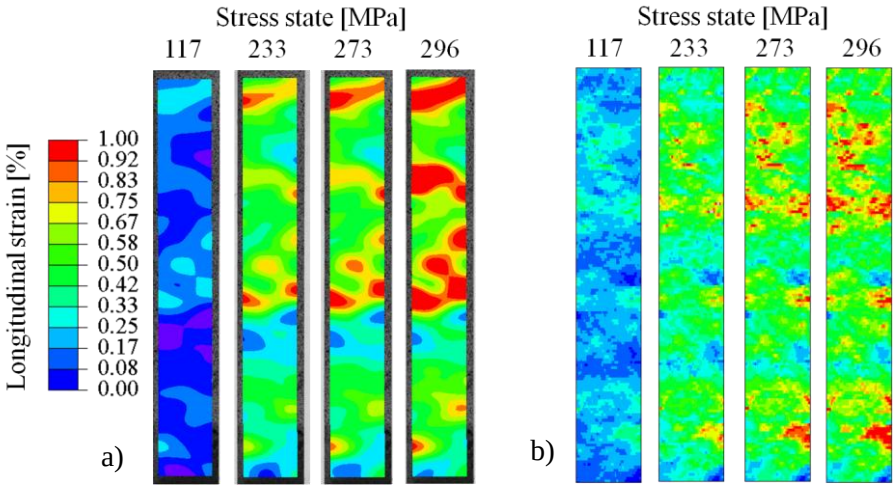

Figure 6. Evolution of the strain-field captured with a) DIC and b) FE model

Comparison between the measured and the calculated global modulus is shown in Figure 7a. Both sets of data indicate that modulus is variable among specimens (tested or simulated), as shown by the error bars in Figure 7a. The model predicts well the modulus of ROS composites with longer strands and over-predicts for composites with shorter strands. Some of this discrepancy can be explained by the fact that smaller strands are more prone to be oriented out-of-plane, and hence have lower in-plane modulus. In the future, a knockdown factor could be incorporated in the model to reduce the in-plane material properties based on the probability of out-of-plane strand orientation.

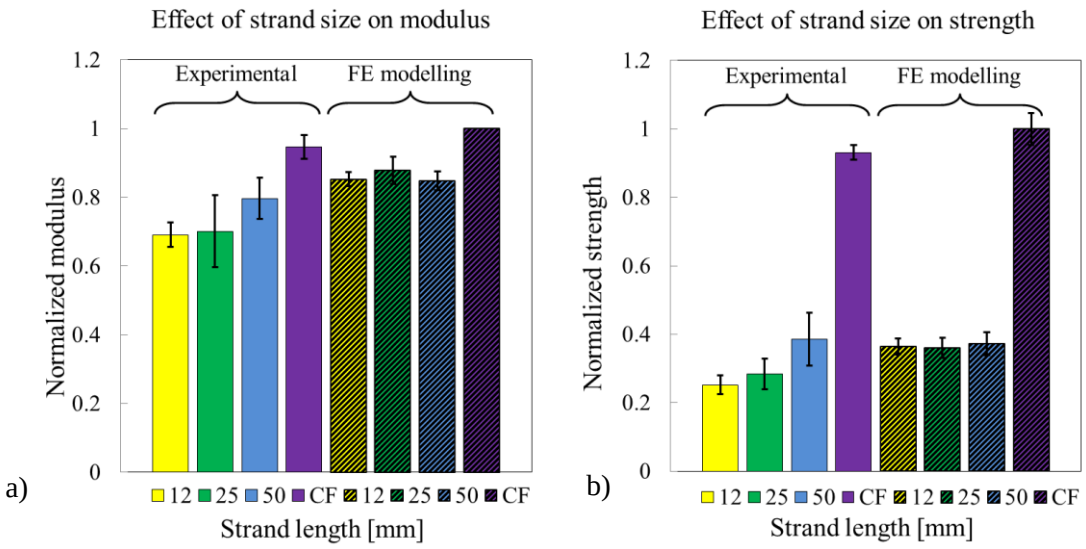

Figure 7. The effect of strand length on a) modulus and b) strength. Error bars show the standard deviation

Measured and predicted strengths of ROS composites are summarized in Figure 7b. Values were normalized by the strength of CF quasi-isotropic laminates predicted by FE models. Overall, strength obtained with ROS panels is less than 40% of the strength of CF quasi-isotropic laminates. Two possible explanations for the large reduction in strength are material heterogeneity and matrix-dominated failure mode. Examination of the cross-sectional micrographs of failed specimens showed that little damage developed away from the main fracture region, signifying that specimens failed at the weakest point while the rest of the specimen was still intact. Similar results were obtained through simulation. For instance, Figure 8 shows progressive failure of an FE specimen in terms of the evolution of Hashin's a) matrix tension and b) fibre tension criteria. Only the first ply is shown, but it is representative of the general state of the entire specimen. There are a few regions with extensive matrix damage, but little fibre damage can be detected. It is evident that failure is localized, while a large portion of the specimen remains undamaged. Strength of ROS composites is highly variable and even FE simulations predicted a wide range of failure loads, as shown by the error bars in Figure 7b. The modelling technique proposed in this paper captures the non-uniform damage development within a specimen as well as a difference in load bearing capacity among them.

Experiments show that this material fails due to interlaminar shear between the strands; however, the current model is a simple 2D case, which does not capture delamination. Nonetheless, both simulation and tests show that fracture is a matrix dominated event, whether it is matrix tension or shear, which explains why the strength is low. As stated in the introductory sections the main goal of the paper was to develop a modelling technique that would capture the heterogeneity of ROS composites. From an industrial standpoint, variability is an important parameter since it is involved in the calculation of design allowables. The modelling method proposed herein is a stepping stone in developing tools for prediction of properties of ROS composites, and it will be improved in the future to incorporate interlaminar shear.

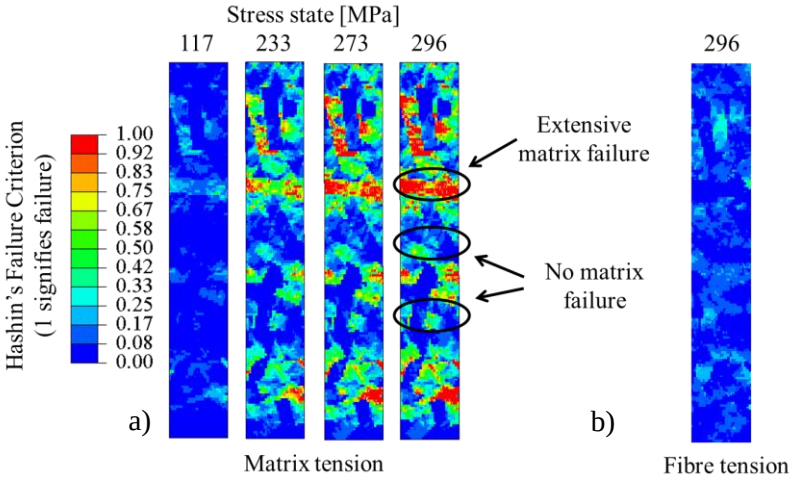

Figure 8. Progressive failure depicted by Hashin's a) matrix tension and b) fibre tension failure criteria, where the value of "1" signifies failure

Results presented thus far were based on partition and mesh size of 1 mm. To analyze the sensitivity of the model to these parameters, the same set of strand orientations and positions were used to generate FE specimens with partition size of 0.5, 1, 2 and 3 mm, and with mesh size ranging from 0.5 to 3 mm. All the models regardless of partition or mesh size showed the same features on the stress and strain plots and predicted the same modulus. The only difference among the strain plots is that larger partition size resulted in a coarser pattern. It was found that partition size affects the computer's ability to converge. Over ten runs, average normalized strength predicted using partition size of 0.5, 1, 2 and 3 mm was 0.33, 0.35, 0.37 and 0.41, respectively. It is hard to select the best partition size based on these results, but overall the estimated strength of ROS composites is still significantly lower than that of CF laminates.

6. Conclusion and future work

Experimental and modelling results showed that strength and modulus of ROS composites vary from one specimen to another due to the heterogeneity of the material. Also, ROS composites fail at relatively low loads in comparison to CF laminates, mainly because failure occurs based on the weakest-link principle and is matrix-dominated. Actual specimens fail due to delamination between the strands, and FE specimens fail due to matrix tension based on Hashin's failure criteria. The main downfall of the model is that it does not capture interlaminar shear and delamination, dominant factors influencing strength of the shorter strands. Hence, the main focus of future work will be to incorporate both factors into the model. Overall, the stochastic approach presented in this paper can successfully capture the heterogeneity of strength and stiffness of ROS materials, and it can be implemented into more complex strength models or adapted for other purposes, such as modelling of thermal residual stresses.

Acknowledgements

The authors would like to greatly acknowledge financial support provided by McGill University and the industrial partners: Bell Helicopter Textron Canada Limited, Bombardier Inc., Pratt and Whitney Canada Corp., Marquez Transtech Limited, Delastek Inc. and Avior Integrated Products Inc. The authors would also like to acknowledge the funding provided by the Natural Sciences and Engineering Research Council (NSERC) and the Consortium for

Research and Innovation in Aerospace in Quebec (CRIAQ). Finally, the authors would like to acknowledge the National Research Council of Canada for providing the facilities, equipment and assistance with fabrication and preparation of the specimens.

References

[1] N. Eguémann, *et al.*, "Compression moulding of complex parts for the aerospace with discontinuous novel and recycled thermoplastic composite materials " in *The 19th International Conference on Composite Materials*, Montreal, Canada, 2013.
[2] M. Selezneva, *et al.*, "Compression moulding of discontinuous-fibre carbon/PEEK composites: study of mechanical properties," in *SAMPE*, Baltimore, 2012.
[3] M. Selezneva, *et al.*, "Mechanical properties of randomly oriented strands thermoplastic composites," in *The 19th International Conference on Composite Materials* Montreal, Canada, 2013.
[4] G.-P. Picher-Martel and P. Hubert, "Squeeze flow behaviour of Carbon/PEEK Randomly-Oriented Strands under transverse compaction," in *American Society for Composites 27th Annual Technical Conference/The 15th US-Japan Conference on Composite Materials*, Arlington, Texas, US, 2012.
[5] G.-P. Picher-Martel, *et al.*, "Squeeze flow of randomly-oriented strands thermoplastic composites," in *The 19th International Conference on Composite Materials*, Montreal, QC, Canada, 2013.
[6] B. Landry and P. Hubert, "Processing effect on the damage tolerance of randomly-oriented strands thermoplastic composites," in *The 19th International Conference on Composite Materials*, Montreal, QC, Canada, 2013.
[7] J. H. Han, *et al.*, "Effect of fabric reinforcement on failure response of discontinuous long fiber composite bolted joints," in *SAMPE* Long Beach, CA, 2011.
[8] P. Feraboli, *et al.*, "Modulus measurement for prepreg-based discontinuous carbon fiber/epoxy systems," *Journal of Composite Materials*, vol. 43, pp. 1947-1965, September 1, 2009 2009.
[9] P. Feraboli, *et al.*, "Notched behavior of prepreg-based discontinuous carbon fiber/epoxy systems," *Composites Part A: Applied Science and Manufacturing*, vol. 40, pp. 289-299, 2009.
[10] P. Feraboli, *et al.*, "Characterization of prepreg-based discontinuous carbon fiber/epoxy systems," *Journal of Reinforced Plastics and Composites*, vol. 28, pp. 1191-1214, May 1, 2009 2009.
[11] T. Matsuo, *et al.*, "Design and manufacturing of anisotropic hollow beam using thermoplastic composites," in *The 19th international conference on composite materials*, Montreal, Canada, 2013.
[12] Y. Sato, *et al.*, "Elastic modulus estimation of chopped carbon fiber taper reinforced thermoplastics using the monte carlo simulation," presented at the The 19th international conference on composite materials, Montreal, Canada, 2013.
[13] P. Feraboli, *et al.*, "Stochastic laminate analogy for simulating the variability in modulus of discontinuous composite materials," *Composites Part A: Applied Science and Manufacturing*, vol. 41, pp. 557-570, 2010.
[14] "21.3.2 Damage initiation for fiber-reinforced composites," in *Abaqus/Standard v. 6.10. Abaqus Analysis User's Manual* ed.
[15] "21.3.3 Damage evolution and element removal for fiber-reinforced composites," in *Abaqus/Standard v. 6.10. Abaqus Analysis User's Manual* ed.
[16] M. Naderi, "Stochastic analysis of inter- and intra-laminar damage in notched PEEK laminates," *eXPRESS Polymer Letters*, vol. 7, pp. 383-395, 2013.